



Enhancing Power Plants Safety by Accurately Predicting CO and NO_x Leakages from Gas Turbines Using FFNN and LSTM Neural Networks

Samar Taha Yousif¹, Firas ALNAIMI^{2,*}, Ammar Al Bazi³, and Sivadass THIRUCHELVAM⁴

¹ Universiti Tenaga Nasional, College of Engineering, 43000 Kajang, Selangor, Malaysia

¹ University of Information Technology and Communications, College of Engineering, Baghdad, Iraq

² Universiti Tenaga Nasional, Institute of Power Engineering, Power Generation Unit, 43000 Kajang, Selangor, Malaysia

³ Aston University, College of Business and Social Sciences, B4 7UP, Birmingham, UK

⁴ Universiti Tenaga Nasional, Institute of Energy Infrastructure, 43000 Kajang, Selangor, Malaysia

*Corresponding author. firas@uniten.edu.my

Abstract

Gas power plants are fast-establishing power plants capable of producing reliable energy in high watts volumes. One of its significant features is its dependency on natural air as raw material to run the gas turbine. Air passes through several stages that involve heating the air to increase its pressure before being used in electric power generation. Leakage in gas power stations is considered a vital indication of irregular processes of those stages. Any fault existing in the meanwhile operations can result in lousy production performance. Considering the human and economic losses of gas leakage, it has become a challenge to prevent the same. One of the essential approaches to managing gas leakage reduction is an accurate prediction. This paper proposes an automatic prevention approach relying on deep learning technology for predicting gas leakage status.

Furthermore, a novel dataset was supplied by a natural gas power plant to predict CO and NO_x emissions. The dataset is used to train the deep learning models using Long-short Term Memory and Feed-Forward Neural Networks. The optimum accuracy obtained is over 92% for CO and over 58% for NO_x while using the LSTM model as a predictor.

Keywords: Gas Leakage, FFNN, LSTM, Deep Learning

1. Introduction

A gas turbine converts air into a high-temperature and high-pressure gas to spin a turbine engine (Li & Ying, 2018). For electricity production, thermodynamic energy is transformed into mechanical energy. Power production in a gas-fired power plant (GPP) involves three basic components: gas compressor, combustor, and turbine (Li & Ying, 2018). Another important

process in a gas turbine is generating combustion energy, which is used to heat the alleged working gas. The GPP's combustion chamber significantly compensates for the energy lost when the working gas leaves the compressor (Yazdani et al., 2020). A gas turbine's performance quality is determined by a number of considerations related to the operation of each GPP component. Many researchers focus on enhancing gas turbine performance, mostly by



enhancing the pre-turbine process (in the compressor and combustor part). The incoming air is cooled before entering the compressor to enhance the power output at the high ambient temperature (Liang et al., 2020). From this point, performance-enhancing technologies were introduced, employing mechanical coolers to cool the air before it was sent to the compressor. It is important to note that employing a chiller has significant operational costs; as stated in (Bao et al., 2019), it accounts for 30% of the electricity generation cost. Another disruptive and performance-decreasing factor is turbine exhaust. According to (Bao et al., 2019), gas emissions depend on the ambient temperature of the intake air; it has been reported that the turbine's carbon emissions rise as the ambient input air temperature decreases. As reported by (Bao et al., 2019), gaseous emissions (i.e. carbon) depend on the fuel utilized in the combustion process. This paper presents a cost-effective alternative to improve output power quality and reduce pollution levels from gas turbine emissions. Since gas emissions are related to many aspects of turbine performance and quality, such as ambient inlet and outlet air temperature, ambient air pressure, ambient humidity, etc. Once emissions are successfully predicted, troubleshooting can be done to prevent future damage. In this paper, natural gas turbines are preferred because of their lower gas emission levels than diesel and petroleum fuels (Bao et al., 2019). In most countries, GPP is a fast and efficient alternative for generating electricity. In any power plant, safety and risk prevention studies are a must and must be carried out regularly to prevent unfortunate events. A large number of generating cooperatives and companies are conducting safety information studies. Take the example of a gas-fired power plant; gas leaks greatly impact human and property resources. According to (Matjanov, 2020), gas-fired power plants are located near residential and industrial areas, and there is a high risk of fire or explosion in the event of a gas leak. Risks of gas leaks/emissions may include poisoning, fire and impaired machine performance (Kwon et al., 2018). In 2003, a gas eruption occurred in Kaixian Town, China County, killing 243 people and evacuating 100000 people (Hashmi et al., 2020). In (Guteša Božo et al., 2019), intelligent systems for monitoring city air pollution are being developed because of gas-fired power plants. Traditional monitoring systems that rely on humans to diagnose and report errors are no more keeping pace with the energy system's massive development. The use of semiconductor-based sensors for detecting gas leaks has a number of drawbacks, including low gas sensitivity (Caposciutti et al., 2020). Optical sensors have also been used for the same purpose, especially since light-emitting diode (LED) technology became commonplace. Unfortunately, due to their limited temperature and pressure tolerance, LED sensors are very prone to explosion, causing reliability issues when used in

critical applications such as gas turbines (Majdi Yazdi et al., 2020). An approach was presented by (Sanchez et al., 2018) relying on wireless sensor networks (WSN) for gas leak detection using wearable sensors integrated into worker/employee suites. Wireless sensors are energy efficient and can be used in harsh environments, but this idea remains the limit of human availability and willingness to monitor processes inside gas turbines. Leakage event predictions depend on historical data from conventional gas turbine sensors and have been implemented in many studies as prior art. However, gas leak prediction (proactive control) and traditional/continuous monitoring activities support its results. It has not proven itself as an independent monitoring alternative for gas-fired power plants (Volponi, 2014). Computer vision methods such as neural networks have been used as the backbone of proactive emission monitoring methods in research, and the first research on the prediction of gas emissions based on neural networks can be traced back to 1999 (Lu et al., 2018). As described by (Aliramezani et al., 2020), Support Vector Machine (SVM) model was used to predict gas emissions such as (NO_x) from gas turbines and diesel engines. Perform NO₂, CO₂, SO₂ and O₃ emissions prediction using LSTM model in Bangladesh (Karim, 2023). However, they have a disadvantage when choosing features, which can lead to erroneous output if done by trial and error. Classification and prediction of emissions from different fuels were performed using the support vector machine (SVM) and Artificial Neural Network (ANN) (Tuttle et al., 2020). An Extreme Learning Machine (ELM) has been used to predict the intensity of carbon emissions in some cities (Sun & Huang, 2022). In (AlKheder & Almusalam, 2022), a deep FFNN model was used for predicting CO₂ emission amounts from a specific power sector in Kuwait. Deep Neural Network (DNN) and SVM models were effectively implemented in (Production, 2022), to predict CO₂ emission in Tukey. Linear and nonlinear prediction methods are used for forecasting energy demand in (Wang et al., 2018), and it was subsequently pointed out that nonlinear predictors did not provide a significant increase in forecast accuracy compared to linear predictors.

This paper proposes two artificial intelligent models, namely Feed-Forward Neural Network (FFNN) and Long Short Term Memory (LSTM), to capture the emission of two gases, Carbon monoxide (CO) and Nitrogen oxides (NO_x). These models were developed using a dataset collected in 5 years (2015 – 2019), representing the largest dataset gathered for this topic. An active method relying on computer vision and deep learning paradigms is developed to predict gas emissions. Once emissions can be accurately predicted, troubleshooting may be done to avoid further damage. The substance of this paper is

structured as follows: In the following section, the required steps for power production and causes of gas leakage in a gas power plant are discussed. Section 3 introduces the collected data set with the statistical analysis of its features. Section 4 describes the proposed prediction models. The experimental results are presented in Section 5. Results are discussed in section 6. The conclusion and further research direction were presented in the last section.

2. Gas power plant

The gas power plant is among the high-performance power stations in terms of production and cost. It is reported that gas power plants can be constructed faster than other plants, which is the best option for urgent demands. Those plants use the air as raw material and heat power as a helping factor. The power generation process in gas power plants ends by turning the turbine (gas turbine) blades and maintaining it to run in stable performance. The following steps are considerable during the power production of gas power plants:

1) air (normal air) is processed through the air filter to eliminate the dust and other associates mixed with air. Air is required to be passed to the upcoming stage with high pressure. Thus, the compressor is used for increasing the air pressure; say, at the compressor, inlet air is provided at low pressure, and its outlet air is reproduced with high pressure.

2) many researchers insist that using a cooling system before the compressor increases the air pressure. Hence, the cooling system is essential for pressure performance enhancement; it has been adopted in gas power plants.

3) as stated above, the gas turbine deploys two raw materials to generate electrical power. Those materials are natural air and heat energy from fuel ignition. Subsequently, the regenerator inlet air is provided at high and low temperatures, and its outlet air is reproduced with high pressure and temperature. In the next stage, after the air compression, air regeneration takes place, which involves heating the high-pressure air. The heating process passes this highly pressured air through a network of fine tubes (heat exchangers). Those fine tubes are exposed to hot gases, usually hung over from the upcoming stages in the gas turbine. This gas is termed as exhausted gas and feedback from the other process of the gas power plant.

4) The air enters the compensation chamber at high pressure and temperature. However, burnable fuel is resided in this chamber and is meant to overheat the incoming air to a very high

temperature, i.e. 3000 degrees (F). Gas power plants utilize oil fuel for heating purposes, and this stage is encountered exhaust gases that result after passing the very hot air into temperature mitigation rooms. Those exhausted gases are feedbacked to the regenerator stage (point 3).

5) the final voyage of the air ended with temperature mitigation after the air passed out from the compensation chamber. Temperature is mitigated from 3000 degrees (F) to 1500 degrees (F) which is proved to be a suitable temperature for turning off the gas turbine (alternator). Figure 1 demonstrates all the mentioned stages.

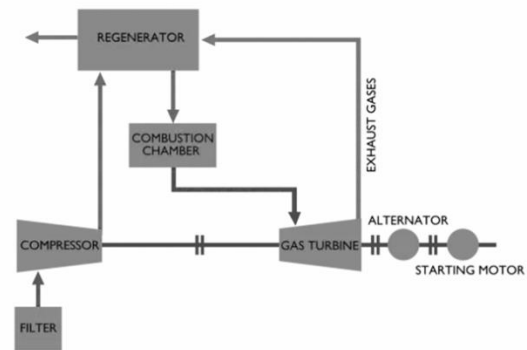


Figure 1. Gas turbine flow diagram illustration of air journey

In order to study the causes and impact of gas leakage in the gas turbine, the following points are brought up as the main motivations behind the study:

a. gas leakage is health damaging, considered the leading cause of organ cancers, i.e. lung and skin cancer. More leakages cause instant death due to gas poisoning, which makes the major power industry life-risking.

b. technically, a gas power plant is similar to other traditional power generation plants, such as diesel power plants, etc., in terms of running cost. Every kilowatt of electrical power has a particular cost involving fuel and other operational costs. Gas leakages lead to performance dropping, which impacts power generation.

It can be concluded that preventing leakage may save both lives and costs, and it is proposed that proactive measure is essential in preventing gas leakages. This approach is made using gas leakage prediction based on historical leakages of the power plant. In order to implement this approach, the following prerequisites are mandatory: Adoption of an intelligent method for prediction tasks. This presents two approaches: the analytical approach, including likelihood methods, hidden Markov model, Bayesian rules, etc., and the computational approach that relies on computer vision programs in prediction tasks. The first approach (analytical prediction) is associated with high computation budget and forces another cost

during its adoption. Subsequently, the computational approach outperformed and was selected for prediction implementation. Significant data availability is essential for working with intelligent prediction models. This data is obtainable from monitoring and logging information recorded for an extended period in the same power plant. However, data adaptation from other power plants for implementing a prediction model cannot stand in terms of prediction accuracy. Dealing with the supervised problem is required obtaining data related to the same problem space to ensure precision in prediction.

3. Dataset description

The dataset is collected from a natural gas power plant near Baghdad's northern border to build the prediction model. The gas leakage level from the turbine entities is after that termed as the number of gas turbine emissions. The emission of poisonous gases from the said gas turbine was monitored using nine sensors to detect the emission of NO_x and CO from the turbine corpus. Data is being broken down for hourly readings from each sensor. In other words, a sensor reading for an hour is accumulated into one reading by applying a sum or average to all readings. Besides, This dataset is collected for five years with a total of 39677 hours. Data includes gas turbine parameters (temperature and pressure) and ambient variables. Each sensor is used to determine specific features. Table 1 prescribes the general characteristics and descriptive statistical analysis mentioned in the dataset. The data is gathered within a range of operations between 70% for a partial load and 88% for a full load. After one year of monitoring data, statistical analysis is performed to study the CO and NO_x leakage level, and the results in Table (2) are achieved. The maximum leakage level of CO and NO_x gases was obtained at 45.2761mg/m³ and 71.808 mg/m³, respectively, while the minimum leakage level was 0.27664 mg/m³ and 11.543 mg/m³, respectively. The median and mean of CO and NO_x leakage levels are measured too. CO and NO_x are demonstrated by histogram as in Figure 2. Figure 3 shows the gas turbine's schematic diagram used in the paper, where the sensing and monitoring system in the gas turbine shows the values of continuous, real-time parameter sensing and monitoring for the data centre.

	AAT	CIP	RH	TIDP	EP	CIT	ET	TE	CDP
CO	-	0.12	0.02	-0.03	-	-0.12	0.05	-	-
	0.07				0.07			0.003	0.06
NO _x	-	0.53	0.43	-0.29	-	-0.14	-	0.001	0.001
	0.57				0.02		0.18		

Table 1. Emission sensing information (variables) used for the prediction approach

Variable	Annotation	Unit	Min.	Max.	
Ambient Temperature	Air	AAT	°C	0	49.9

Compressor Inlet Pressure	CIP	mbar	991.2	1033
Relative Humidity	RH	%	12	100
Turbine Inlet Discharge Pressure	TIDP	mbar	4.17	15.22
Exhaust Pressure	EP	mbar	15.92	37.60
Compressor Inlet Temperature	CIT	°C	800.64	889.48
Exhaust Thermocouple	ET	°C	408.83	440.48
Turbine Energy	TE	MWH	70.72	111.96
Compressor Discharge Pressure	CDP	mbar	11.84	18.19

Table 2. CO and NO_x emission levels value analysis

	Min	Max	Med	Mean
CO	0.27664	45.2761	3.49011	4.586391966
NO _x	11.543	71.808	34.4646	36.550022

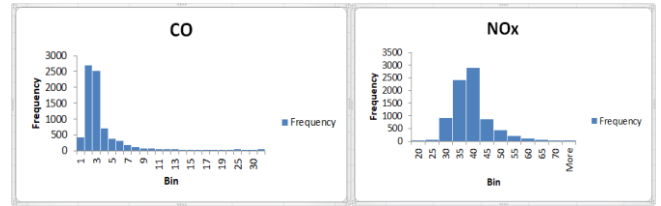


Figure 2. Histogram representation of CO and NO_x emissions

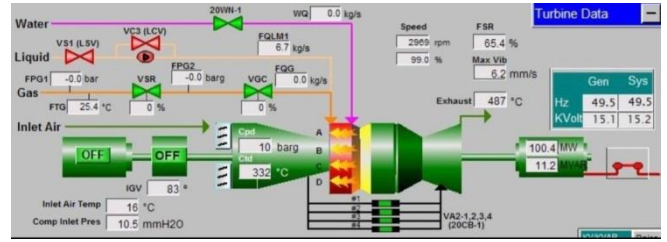


Figure 3. The turbine data

Figure 2 above revealed that CO emission volume was 2 mg/m³ to 4 mg/m³. Similarly, NO_x emission volumes in the range of 30 mg/m³ to 40 mg/m³ are the highest among recorded emissions.

In order to demonstrate the linear relationship between dataset features and the emissions of CO and NO_x gases, Pearson correlation (Equation 1) is obtained between each feature and gas emission values; the same is demonstrated in Table 2.

$$P.C. = \frac{\sum(x_i - x')(y_i - y')}{\sqrt{\sum(x_i - x')^2 \sum(y_i - y')^2}} \quad (1)$$

Wherein,

P.C. represents the Pearson correlation coefficient, x_i represents the values of the x-variable sample, x' represents the mean of the x-values variable, y_i represents the values of a sample's y-variable, y' represents the mean of the x-values variable.

Table 3. Pearson correlation between the dataset features and the targets/gases emission

Table 3 revealed that Exhaust Thermocouple (ET) has a very weak linear relationship with the emission volumes of CO, whereas Compressor Inlet Temperature (CIT) has the strongest linear

relationship. On the other hand, Turbine Energy (TE) and Compressor Discharge Pressure (CDP) have a very weak linear relationship with NO_x emission volumes. In contrast, Ambient Air Temperature (AAT) has the strongest relationship.

4. Prediction models

The core objective of this section is to highlight the internal sections (participants) of the prediction paradigm and the measures taken to optimize the model's performance. The prediction model consists of two stages: training and testing. During the training stage, data in high volumes are fed into the model, which is tuned up for mapping those data into the appropriate target. Deep learning classifiers are being used to implement such a model: FFNN and RNN/LSTM. Figure 4 Outlines the required steps for the prediction model.

It was knowing that data fusion, normalization, and feature selection (Pearson Correlation) are meant to enhance prediction accuracy. Moreover, K-fold cross-validation was used to avoid model overfitting, in which the data was partitioned into 10 folds. Then, the model was repeatedly trained on nine folds, with the last holdout fold serving as the test set. In order to overcome the variance in the dataset, the min-max feature scaling technique was used, where all dataset values were changed to a (0-1) scale without losing information. The accuracy can be calculated as per the below equation:

$$ACCUR = \frac{\text{Number of correct decisions}}{\text{Total number of outputs}} \quad (2)$$

To understand the distribution of errors in the classifier results, mean square error (MSE) is calculated, which describes the error between predicted and actual values by providing the average of the square error. However, mean absolute error (MAE) and root mean square error (RMSE) are evaluated for more abstraction of error understanding. The MAE provides a smaller in-value output than the MSE value, revealing the prediction error amount. Similarly, RMSE is meant to downscale the MSE value into smaller values (see Equations 3,4 and 5).

$$MSE = \frac{\sum_{n=1}^i e(n)^2}{i} \quad (3)$$

$$MAE = \sum_{n=1}^i \frac{|e[i]|}{i} \quad (4)$$

$$MSE = \sqrt{\frac{\sum_{n=1}^i e(n)^2}{i}} \quad (5)$$

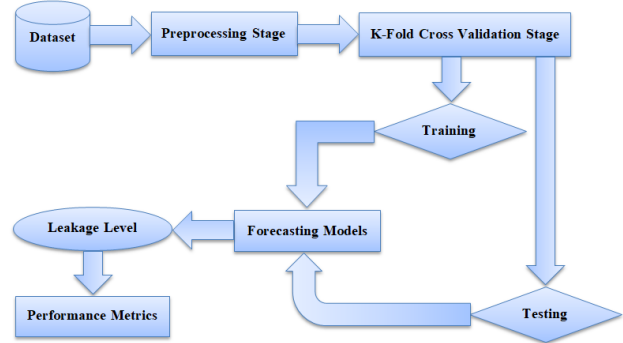


Figure 4. Outlining of the prediction model, including the preprocessing and post-processing paradigms

4.1. FFNN

Feed-forward neural networks (FFNNs) are known for their ability to learn complex problems and provide solutions by learning hidden structural relationships of input strings (Lemma & Hashim, 2012). For the simple single hidden layer FFNN (net) shown in Figure 5, supervised learning must be provided by using the inputs vector $r=[r_1,r_2,r_3,\dots,r_i]$ and targets vector $T=[T_1,T_2,T_3,\dots,T_i]$. Errors are identified by correlating the resulting and target vectors (Equation 6). The weight coefficients (W) between layers can be adjusted to meet the minimum error output (Jiao et al., 2011).

$$R = net(r) \quad (6)$$

$$R = W \times r + b \quad (7)$$

R is the output vector, r represents the random variable, and b is the model bias. Therefore, the net can adjust the W coefficient to achieve the best correlation between R and T (Zhang et al., 2006). In other words, the learning process is to find the minimum of equation (3).

$$e = R - T \quad (8)$$

e is the error vector, a measure of training/learning performance (Yu et al., 2011).

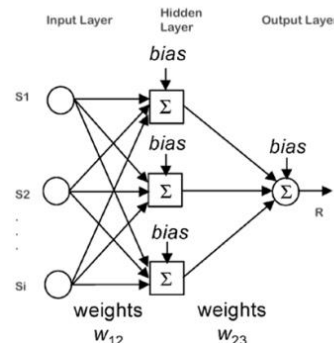


Figure 5. The input, weights, biases, and output are displayed in the FFNN layer structure

Net is trained on guessing the gas leakage level. The prediction model begins with baseline development using a feedforward neural network classifier. The model size and the number of iterations were adjusted to dramatically improve the classifier's performance, as listed in Table 4. FFNN is realized by allotting the weight coefficients randomly to the neurons. That impacts the output quality; varying output is yielded from the model of mentioned settings.

Table 4. Baseline standard FFNN model

Parameter	Value
Number of hidden layers	Single (1)
Goal training performance (MSE)	$1 \times e^{-201}$
Training model	Levenberg–Marquardt algorithm
Minimum gradience	$1 \times e^{-1}$
Maximum fails	10
Epochs	22
Training time goal (seconds)	1

4.2. LSTM

LSTM networks are a common type of neural network that uses the backpropagation training technique. LSTMs are constrained to be recurrent neural networks in which data predictions depend on previous predictions of the same data. For example, using the RNN network to predict the next word in a speech sequence (sentence) depending on the preceding word in the same context (Kwon et al., 2018) (Safiyullah et al., 2018).

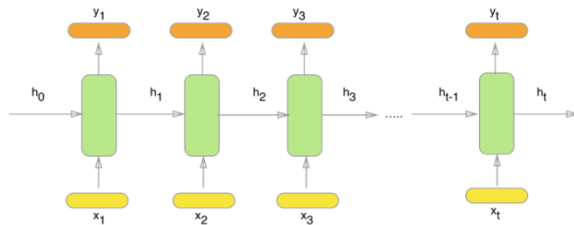


Figure 6. RNN structure

Considering the illustration in Figure 6, the expectation of the upcoming word in a spoken sentence (t) contains multiple words. Every word is portrayed as x_1, x_2, x_t , and the input word is fed into (t) multiple training models. A singular neural network is trained separately using the input provided and produces an output as y_1, y_2, y_3 , and y_t . In the RNN network, the subsequent output prediction depends on the preceding neural network's output and updates the subsequent model training process by generating coefficients such as h_1, h_2, h_3 , and h_t , etc. It is difficult to achieve the desired accuracy out of RNN because of the vanishing gradient problem, which cancels out the training accuracy. To solve this issue, LSTM is designed to combat the gradient vanishing problem

via a gating mechanism, as shown in Figure 7.

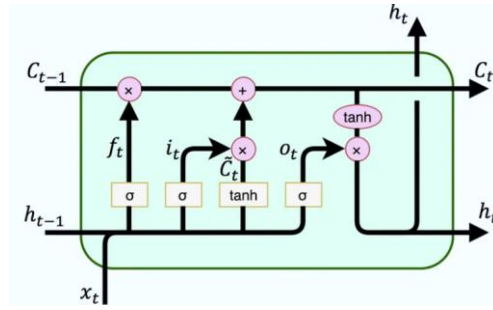


Figure 7. LSTM internal structure

LSTM neural networks are designed to address learning errors and interruptions in training, especially when the data changes. The model starts by defining input arrays, which could be data and target arrays. However, in a neural network with long short-term memory, there is no need to define the data as a horizontal or vertical representation. Data can be entered in rows and columns, and targets can be regular arrays represented by rows or columns.

A point of contention is determining the number of hidden layers that affect the model's overall performance. In this paper, various hidden gates were tested to meet different performance requirements, such as scaling downtime or improving accuracy. We ended up with two hidden gates that made timing and accuracy as required.

5. Results and discussions

The overall accuracy and performance metrics results of CO and NO_x emission prediction using the FFNN model and 10-fold cross-validation were obtained. The performance of each fold is represented independently in Table 5.

Table 5. k-fold cross-validation, accuracy, and performance metrics for flue gas emission prediction using standard FFNN model. The best results are shown in bold.

Table 5 shows that the best results for CO and NO_x are obtained on the 6-fold and 5-fold cross-validation, respectively. Furthermore, MSE is the biggest value, and RMSE is almost half the values of the MSE, which validates the formulas of MSE and RMSE given previously.

On the other hand, LSTM is used for predicting the emission of CO and NO_x gases, and the prediction results are given in Table(6).

Table 6. Accuracy and performance metrics for flue gas emission prediction using the LSTM model

Metric	CO Prediction Performance	NO _x Prediction Performance
Accuracy	92.9979	58.2165
MSE	0.3094	0.8357
RMAE	0.5562	0.9141
MAE	0.4323	0.7553

The scatterplots shown in Figures (8) and (9) demonstrate a perfect correlation of predicted values against observed ones. According to the above Table, the LSTM model outperformed the FFNN model by 61.52 percent for CO gas prediction accuracy and 65.58 percent for NO_x gas leakage prediction accuracy. Furthermore, the LSTM prediction model performs more acceptably because the predicted values overlap entirely with the total number of observed cases.

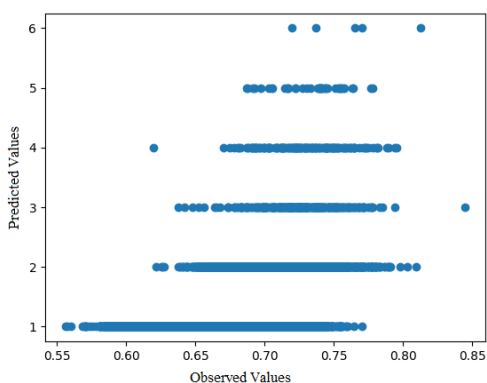


Figure 8. Scatterplots for the LSTM prediction model (CO emission)

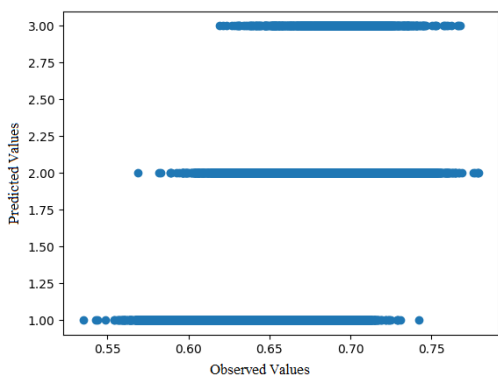


Figure 9. Scatterplots for the LSTM prediction model (NO_x emission)

Fold No.	CO Prediction Performance				NO _x Prediction Performance			
	ACC.	MSE	RMSE	MAE	ACC.	MSE	RMSE	MAE
1	34.5	5.34	2.709	2.56	19.7	3.70	1.949	0.12
2	35.2	5.34	2.709	2.56	19.7	3.70	1.950	0.12
3	34.2	5.34	2.710	2.56	19.8	3.72	1.909	0.12
4	34.5	5.31	2.705	2.55	19.6	3.79	1.941	0.12
5	34.2	5.32	2.705	2.56	20.0	3.55	1.936	0.12
6	35.7	5.29	2.701	2.55	19.6	3.68	1.942	0.12
7	34.0	5.30	2.702	2.55	19.6	3.67	1.937	0.12
8	34.7	5.32	2.706	2.55	19.6	3.67	1.937	0.12
9	35.0	5.33	2.708	2.56	19.7	3.70	1.949	0.12
10	33.5	5.38	2.717	2.57	19.8	3.71	1.958	0.12

6. Conclusions

Predicting gas leakage in gas power plants is considered a challenging task vital for workers' safety, environments, and economic system. Two main gases are dominant in this paper, namely CO and NO_x. Considering the poisonous impact of those gases and their correlation with the internal gas turbine process and generation performance, inventing a cost-efficient and reliable technique for combating such leakages becomes essential. According to the results above, the following points can be concluded:

(a) Results show that the accuracy of the prediction of CO gas leakage is greater than that of the prediction of NO_x gas leakage. That difference in accuracy is measured to be 44.01 percent in the FFNN model and 37.4 in the LSTM model, favouring CO gas leakage prediction that leads to the accuracy over the NO_x gas leakage prediction.

(b) Both accuracies of prediction gas leakage in standard FFNN are in low grade; the maximum accuracy is 35.7852 percent, while in the LSTM model, the accuracy reached 92.9979 percent for CO and 58.2165 for NO_x.

(c) The performance gap in predicting the CO and NO_x gas emission can be related to the difference in the amount of leakage (as in Tables 2 and 3). CO gas leakage reached 45.2761, while the NO_x gas leakage

reached 71.808. However, the target (labels) vector of NO_x gas has a maximum number of classes, which applies a computational load on the classifier, hence low-grading the prediction accuracy.

Data availability is the main challenge in this paper. According to the majority of previous research works, own datasets were used. The majority of these datasets are not open-access. This study identified a number of features, techniques, and models that are expected to be evaluated in future work. In addition, other gas emissions can be modeled and predicted using similar test data. Intelligent system models can be applied to power plants to be studied as future emission reduction systems.

References

- Aliramezani, M., Norouzi, A., & Koch, C. R. (2020). Support vector machine for a diesel engine performance and NO_x emission control-oriented model. *IFAC-PapersOnLine*, 53(2), 13976–13981. <https://doi.org/10.1016/j.ifacol.2020.12.916>
- AlKheder, S., & Almusalam, A. (2022). Forecasting of carbon dioxide emissions from power plants in Kuwait using United States Environmental Protection Agency, Intergovernmental panel on climate change, and machine learning methods. *Renewable Energy*, 191, 819–827. <https://doi.org/10.1016/j.renene.2022.04.023>
- Bao, J., Zhang, L., Song, C., Zhang, N., Guo, M., & Zhang, X. (2019). Reduction of efficiency penalty for a natural gas combined cycle power plant with post-combustion CO₂ capture: Integration of liquid natural gas cold energy. *Energy Conversion and Management*, 198(June), 111852. <https://doi.org/10.1016/j.enconman.2019.111852>
- Caposciutti, G., Baccioli, A., Ferrari, L., & Desideri, U. (2020). Impact of ambient temperature on the effectiveness of inlet air cooling in a co-digestion biogas plant equipped with a mGT. *Energy Conversion and Management*, 216(October 2018), 112874. <https://doi.org/10.1016/j.enconman.2020.112874>
- Guteša Božo, M., Valera-Medina, A., Syred, N., & Bowen, P. J. (2019). Fuel quality impact analysis for practical implementation of corn COB gasification gas in conventional gas turbine power plants. *Biomass and Bioenergy*, 122(December 2018), 221–230. <https://doi.org/10.1016/j.biombioe.2019.01.012>
- Hashmi, M. B., Majid, M. A. A., & Lemma, T. A. (2020). Combined effect of inlet air cooling and fouling on performance of variable geometry industrial gas turbines. *Alexandria Engineering Journal*, 59(3), 1811–1821. <https://doi.org/10.1016/j.aej.2020.04.050>
- Jiao, C., Yong-hong, W., & Shi-lie, W. (2011). Application of Wavelet Singular Entropy in Periodic Fault Detection of Sensors on Gas Turbines. *Noise and Vibration Control*, 31(6), 156. <https://doi.org/10.3969/J.ISSN.1006-1355-2011.05.035>
- Karim, R. (2023). An Automated LSTM-based Air Pollutant Concentration Estimation of Dhaka An Automated LSTM-based Air Pollutant Concentration Estimation of Dhaka City , Bangladesh. February.
- Kwon, H. M., Kim, T. S., Sohn, J. L., & Kang, D. W. (2018). Performance improvement of gas turbine combined cycle power plant by dual cooling of the inlet air and turbine coolant using an absorption chiller. In *Energy* (Vol. 163). Elsevier B.V. <https://doi.org/10.1016/j.energy.2018.08.191>
- Lemma, T. A., & Hashim, F. M. (2012). Wavelet analysis and auto-associative neural network based fault detection and diagnosis in an industrial gas turbine. *BEIAC 2012 - 2012 IEEE Business, Engineering and Industrial Applications Colloquium*, 103–108. <https://doi.org/10.1109/BEIAC.2012.6226031>
- Li, J., & Ying, Y. (2018). A Method to Improve the Robustness of Gas Turbine Gas-Path Fault Diagnosis Against Sensor Faults. *IEEE Transactions on Reliability*, 67(1), 3–12. <https://doi.org/10.1109/TR.2017.2695482>
- Liang, Y., Cai, L., Guan, Y., Liu, W., Xiang, Y., Li, J., & He, T. (2020). Numerical study on an original oxy-fuel combustion power plant with efficient utilization of flue gas waste heat. *Energy*, 193, 116854. <https://doi.org/10.1016/j.energy.2019.116854>
- Lu, F., Jiang, J., Huang, J., & Qiu, X. (2018). An iterative reduced KPCA hidden markov model for gas turbine performance fault diagnosis. *Energies*, 11(7), 1–21. <https://doi.org/10.3390/en11071807>
- Majdi Yazdi, M. R., Ommi, F., Ehyaei, M. A., & Rosen, M. A. (2020). Comparison of gas turbine inlet air cooling systems for several climates in Iran using energy, exergy, economic, and environmental (4E) analyses. *Energy Conversion and Management*, 216(May), 112944.

- <https://doi.org/10.1016/j.enconman.2020.112944>
- Matjanov, E. (2020). Gas turbine efficiency enhancement using absorption chiller. Case study for Tashkent CHP. *Energy*, 192. <https://doi.org/10.1016/j.energy.2019.116625>
- Production, S. (2022). Forecasting of transportation-related energy demand and CO₂ emissions in Turkey with different machine learning algorithms. 29, 141–157. <https://doi.org/10.1016/j.spc.2021.10.001>
- Safiyullah, F., Sulaiman, S. A., Naz, M. Y., Jasmani, M. S., & Ghazali, S. M. A. (2018). Prediction on performance degradation and maintenance of centrifugal gas compressors using genetic programming. *Energy*, 158, 485–494. <https://doi.org/10.1016/j.energy.2018.06.051>
- Sanchez, E. Y., Represa, S., Mellado, D., Balbi, K. B., Acquesta, A. D., Colman Lerner, J. E., & Porta, A. A. (2018). Risk analysis of technological hazards: Simulation of scenarios and application of a local vulnerability index. *Journal of Hazardous Materials*, 352(2010), 101–110. <https://doi.org/10.1016/j.jhazmat.2018.03.034>
- Sun, W., & Huang, C. (2022). Predictions of carbon emission intensity based on factor analysis and an improved extreme learning machine from the perspective of carbon emission efficiency. *Journal of Cleaner Production*, 338(January), 130414. <https://doi.org/10.1016/j.jclepro.2022.130414>
- Tuttle, J. F., Blackburn, L. D., & Powell, K. M. (2020). On-line classification of coal combustion quality using nonlinear SVM for improved neural network NO_x emission rate prediction. *Computers and Chemical Engineering*, 141, 106990. <https://doi.org/10.1016/j.compchemeng.2020.106990>
- Volponi, A. J. (2014). Gas turbine engine health management: Past, present, and future trends. *Journal of Engineering for Gas Turbines and Power*, 136(5), 1–20. <https://doi.org/10.1115/1.4026126>
- Wang, Q., Li, S., & Li, R. (2018). Forecasting Energy Demand in China and India : Using Single-linear , Hybrid-linear , and Non-linear Time Series. *Energy*. <https://doi.org/10.1016/j.energy.2018.07.168>
- Yazdani, S., Salimipour, E., & Moghaddam, M. S. (2020). A comparison between a natural gas power plant and a municipal solid waste incineration power plant based on an emergy analysis. *Journal of Cleaner Production*, 274, 123158. <https://doi.org/10.1016/j.jclepro.2020.123158>
- Yu, B., Liu, D., & Zhang, T. (2011). Fault diagnosis for micro-gas turbine engine sensors via wavelet entropy. *Sensors*, 11(10), 9928–9941. <https://doi.org/10.3390/s111009928>
- Zhang, Z., Weng, S. L., & Wang, Y. H. (2006). Application of wavelet analysis in fault diagnosis with gas-turbine sensors. *Dongli Gongcheng/Power Engineering*, 26(2).